# DYNAMIC STABILITY OF A COMPOSITE CANTILEVER BEAM WITH VISCOELASTIC PROPERTIES UNDER A FOLLOWER FORCE

Tae-Woo Kim [1], Ji-Hwan Kim [1]

[1] *Department of Aerospace Engineering, Seoul National University*
*San 56-1, Shinrim-Dong, Kwanak-Ku, Seoul, 151-742, Korea*

**SUMMARY**: The dynamic stability of a composite beam is analyzed numerically considering viscoelastic properties of the material. A cantilever beam made of unidirectional composites under a follower force is taken for the analysis and the influence of the viscoelasticity on the critical load is studied. Assuming the first order shear deformation, the equations of motion are derived from the Hamilton's principle and then the eigenvalue problem is formulated by applying the finite element method wherein the solution is sought through the substitution method.

**KEYWORDS**: dynamic stability, viscoelasticity, composite beam, first order shear deformation, Hamilton's principle, Boltzmann's superposition principle, finite element method, substitution method, critical load

## INTRODUCTION

Composite materials with polymeric matrices are being used to an increasing extent in aerospace structures because of their efficient load carrying capabilities. However, polymeric materials are known to exhibit viscoelastic response, especially at high temperature and moisture, so polymer matrices when used in unidirectional laminates are expected to exhibit strong viscoelastic effects [1]. In particular, properties transverse to the fibers and shear properties are matrix controlled and show strong viscoelastic behavior. Because of the time effects and the peculiar nature in which time enters as a destabilizing parameter, viscoelastic stability problems and the time-dependent effects of materials on dynamic behavior have become more and more important.

During the past decades, not a few stability analyses have been performed based on time dependent materials. Stevens [2] investigated approximately some of the qualitative aspects of the parametric excitation of a viscoelastic column subjected to harmonically varying axial load. He showed that in some cases the instability regions are broadened significantly and shifted toward lower values of the exciting frequencies, as the material becomes more viscoelastic in nature. Plaut [3] studied the stability of a viscoelastic cantilever column subjected to a retarded follower load at its free end, where the destabilizing effect of internal damping and retardation was illustrated. Szyszkowski and Glockner [4] used the dynamic approach to obtain an approximate closed-form expression for the viscoelastic critical load of perfect columns made of linear three elements model materials. Vinogradov [5] presents a theoretical study of the creep-buckling behavior of viscoelastic beam columns under general loading conditions. The general solution is derived by means of the quasielastic method and it is shown that with different loading conditions the magnitude of the axial compressive load typically governs the creep-buckling behavior. Chandiramani et al. [6] dealt with an exact approach to the dynamic stability of orthotropic shear deformable viscoelastic flat plates subjected to in-plane uni/biaxial edge load. In this paper, the nature of instability, by flutter or divergence, was recognized and the influence of various parameters on the analysis was examined. Cederbaum *et al*. [7] analyzed the dynamic stability of viscoelastic laminated plates under a harmonic in-plane excitation by utilizing the concept of Lyapunov exponents.

In the present paper, the dynamic stability of a cross-ply laminated composite cantilever beam under a follower force is investigated numerically considering the viscoelasticity of composite. The equations of motion for the problem are derived from the Hamilton's principle assuming the linear viscoelastic constitutive equations. The stability characteristics are studied for beams with different configuration. And the intensity of instability is examined through the time responses.

## GOVERNING EQUATIONS

Fig.1 shows a composite cantilever beam under a follower force, where *F*, *T* denotes axis in fiber and transverse direction and $\theta_k$ denotes orientation of k-th layer respectively. In the theory of first order shear deformation and linear strain, the displacement field and displacement-strain relationship is expressed respectively as,

$$\begin{aligned} u(x,z,t) &= u_0(x,t) + z\varphi_y(x,t) \\ w(x,t) &= w_0(x,t) \end{aligned} \tag{1}$$

and

$$\begin{aligned} \varepsilon_{xx}(x,z,t) &= u,_x(x,z,t) = u_0,_x(x,t) + z\varphi_y,_x(x,t) \\ \varepsilon_{zx}(x,t) &= w,_x(x,t) + u,_z(x,z,t) = w_0,_x(x,t) + \varphi_y(x,t) \end{aligned} \tag{2}$$

where $u_0(x,t)$, $w_0(x,t)$ represent the displacements at the neutral axis, $\varphi_y(x,t)$ the rotation of a line perpendicular to the neutral axis in z-x plane and $(\;),_a$ the partial derivative with respect to $a$ ($a$: $x$ or $z$). For the constitutive equation, we will use the Boltzmann's superposition principle as linear viscoelastic theory. So the constitutive relations at k-th layer of a laminated beam, with initial strains, can be written as follows [8],

$$\begin{aligned} \sigma_{xx}{}^k(x,t) &= \varepsilon_{xx}(x,0)\{\overline{Q}_{11}{}^k(t) + \overline{Q}_{12}{}^k(t)P_{21}{}^k(t) + \overline{Q}_{16}{}^k(t)P_{61}{}^k(t)\} \\ &\quad + \int_0^t \{\overline{Q}_{11}{}^k(t-\tau) + \overline{Q}_{12}{}^k(t-\tau)P_{21}{}^k(t-\tau) \\ &\quad + \overline{Q}_{16}{}^k(t-\tau)P_{61}{}^k(t-\tau)\}\dot{\varepsilon}_{xx}{}^k(x,\tau)d\tau \\ \sigma_{zx}{}^k(x,t) &= \varepsilon_{zx}(x,0)\{\overline{Q}_{45}{}^k(t)P_{45}{}^k(t) + \overline{Q}_{55}{}^k(t)\} \\ &\quad + \int_0^t \{\overline{Q}_{45}{}^k(t-\tau)P_{45}{}^k(t-\tau) + \overline{Q}_{55}{}^k(t-\tau)\}\dot{\varepsilon}_{zx}(x,\tau)d\tau \end{aligned} \tag{3}$$

where $\overline{Q}_{ij}^k(t)$ is the time dependent modulus at k-th layer referred to *xy* coordinate, with

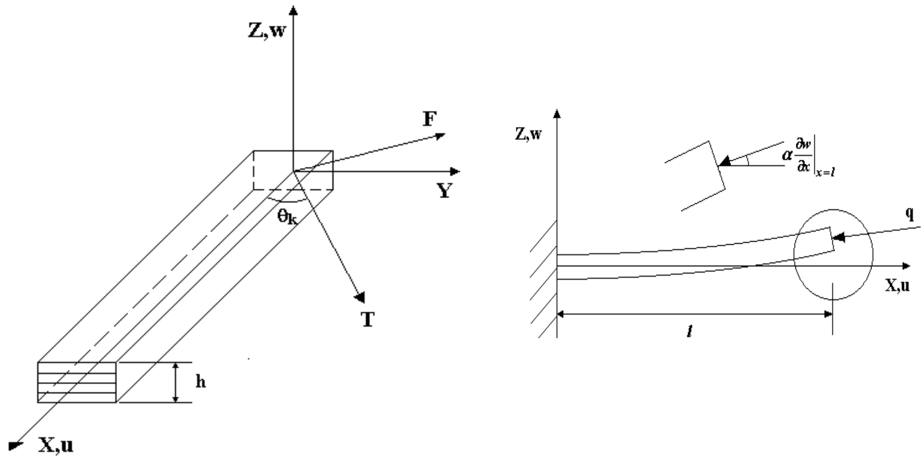


subscripts 1, 2, 4, 5 and 6 denoting *xx*, *yy*, *yz*, *zx* and *xy* respectively, and $P_{21}$, $P_{61}$, $P_{45}$ are Poisson effects[9] which are defined by,

$$
\begin{aligned}
P_{21}^{k}(t) &= \frac{-\bar{Q}_{66}^{k}(t)\bar{Q}_{12}^{k}(t)+\bar{Q}_{26}^{k}(t)\bar{Q}_{16}^{k}(t)}{\bar{Q}_{22}^{k}(t)\bar{Q}_{66}^{k}(t)-\bar{Q}_{26}^{k}(t)^{2}}\\
P_{61}^{k}(t) &= \frac{-\bar{Q}_{22}^{k}(t)\bar{Q}_{16}^{k}(t)+\bar{Q}_{26}^{k}(t)\bar{Q}_{12}^{k}(t)}{\bar{Q}_{22}^{k}(t)\bar{Q}_{66}^{k}(t)-\bar{Q}_{26}^{k}(t)^{2}}\\
P_{45}^{k}(t) &= -\frac{\bar{Q}_{45}^{k}(t)}{\bar{Q}_{44}^{k}(t)}
\end{aligned}
\tag{4}
$$

Now, the equations of motion are derived from the extended Hamilton's principle as in Ref .10,

$$\delta\int_{t_1}^{t_2}(T+W_c)dt+\int_{t_1}^{t_2}(\delta W_{nc}-\delta U)dt=0 \tag{5}$$

where $T$ is the kinetic energy, $\delta U$ the virtual work by internal forces corresponding to the elastic deformation energy, $W_c$ the work done by the conservative portion of the follower force and $\delta W_{nc}$ the virtual work by the non-conservative portion of the follower force. They can be expressed respectively as follows,

$$
\begin{aligned}
T &= \frac{1}{2}\int_A\{I_0(\dot{u}_0^{2}+\dot{w}^{2})+I_2\varphi_y^{2}\}dA, & W_c &= \frac{1}{2}\int_0^l qw_{,x}^{2}\,dx,\\
\delta U &= \int_A\{N\delta u_{0,x}+M\delta\varphi_{y,x}+Qk_s(\delta\varphi_y+\delta w_{,x})\}dA, & \delta W_{nc} &= -\alpha qw_{,x}\big|_{x=l}\delta w
\end{aligned}
\tag{6}
$$

where $N$ is normal force resultant, $M$ moment resultant, $Q$ shear force resultant, $k_s$ shear correction factor, $\alpha$ a parameter that indicates the direction of loading, $A$ cross section area and

$$(I_0, I_2)=\int_{-h/2}^{h/2} b\rho(1,z^2)dz \tag{7}$$

where $\rho$ is density of the material.

In the finite element analysis of beam, the in-plane displacement $u_0$, deflection $w$, and normal rotation $\varphi_y$ can be represented by

$$u_0 = \sum_{j=1}^{m} u_0^j \Phi_j, \quad w = \sum_{j=1}^{m} w_j \Phi_j, \quad \varphi_y = \sum_{j=1}^{m} \varphi_y^j \Phi_j \tag{8}$$

where $u_0^j$, $w_j$ are displacements, $\varphi_y^j$ is rotation at node $j$ and $\Phi_j$ denotes the shape function at node $j$. Substituting Eqn 2, Eqn 3 and Eqn 8 into Eqn 5, one can obtain the following equation in the matrix form,

$$\mathbf{M}\ddot{\mathbf{x}}(t) + \int_0^t \mathbf{K}(t-\tau)\dot{\mathbf{x}}(t)d\tau + \mathbf{W}\mathbf{x}(t) + \mathbf{K}(t)\mathbf{x}(0) = \mathbf{0} \tag{9}$$

where $\mathbf{x}(t)$ is a $m\times1$ global nodal displacement vector, $\mathbf{M}$ a $m\times m$ global mass matrix, $\mathbf{K}$ a $m\times m$ time dependent global stiffness matrix and $\mathbf{W}$ is a $m\times m$ global stiffness matrix from the work by the follower force.

## METHOD OF ANALYSIS

In this paper, the time dependent relaxation moduli $Q(t)$ in the principal material direction is represented by the sum of exponentials, which is practically one of the widely used models for approximation of the viscoelastic behavior of material. Hence, without considering the effects of temperature and moisture they can be given as follows,

$$\begin{aligned} Q(t) &= Q_0 f(t) \\ &= Q_\infty + \sum_{r=1}^{n} Q_r \exp(\beta_r t) \end{aligned} \tag{10}$$

where $Q_0$ and $Q_\infty$ is the modulus at $t$=0, $\infty$ respectively, $f(t)$ is time function which have unity at $t$=0, $\alpha_r$ denotes time constant and $n$ number of time constants for $Q$. We assume that $Q_{11}$ is constant since it is generally controlled by fiber properties, and time function for $Q_{12}$ is equal to the one for $Q_{22}$. Moreover, time function for $Q_{44}$ is taken the same as that for $Q_{55}$ and $Q_{55}$ is supposed to be equal to $Q_{66}$ as in the Ref. 11. Thus relaxation moduli are as follows,

$$\begin{aligned} &Q_{11}(t) = Q_{11}, \quad Q_{22}(t) = Q_{22}^{\infty} + \sum_{r=1}^{n_1} Q_{22}^{r} e^{\beta_{1r} t}, \quad Q_{12}(t) = \frac{Q_{12}^0}{Q_{22}^0} Q_{22}(t), \\ &Q_{44}(t) = Q_{44}^{\infty} + \sum_{r=1}^{n_2} Q_{44}^{r} e^{\beta_{2r} t}, \quad Q_{55}(t) = \frac{Q_{55}^0}{Q_{44}^0} Q_{44}(t), \quad Q_{55}(t) = Q_{66}(t). \end{aligned} \tag{11}$$

Concerning the terms indicating Poisson effect, we discuss cases of cross ply laminated composite beams for constant Poisson effect. Then, at k-th layer, they become:

$$P_{61}^k(t) = P_{45}^k(t) = 0, \quad P_{21}^k(t) = \begin{cases} -\dfrac{Q_{12}^0}{Q_{22}^0} & \theta_\mathrm{k} = 0 \\ -\dfrac{Q_{12}^0}{Q_{11}} & \theta_\mathrm{k} = \dfrac{\pi}{2} \end{cases} \tag{12}$$

Now, the solution of Eqn 9 is sought in the following form as in the Ref. 12:

$$\mathbf{x}(t) = \sum_{j=1}^{m(n+2)} c_j \mathbf{x}_j \exp(p_j t) \tag{13}$$

where $m$ is the degree of freedom and $n$ is the number of distinct time constants in all relaxation moduli, $n_1+n_2$ in this paper. Considering Eqn 11 for three-element solid model, which retains only one exponential term, as each time function $f_1$, $f_2$ one obtains a set of equations for a cross ply laminated beam with zero initial displacement by inserting Eqn 13 into Eqn 9 and performing convolution integral analytically,

$$\{(p_j^2\mathbf{M}+\mathbf{K_0}+\mathbf{W})p_j(p_j-\beta_{11})(p_j-\beta_{21})+\mathbf{K_1}(p_j-\beta_{21})+\mathbf{K_2}(p_j-\beta_{11})\}\mathbf{x}_j=\mathbf{0} \quad j=1,\ 2,\ \ldots,\ 4m \tag{14}$$

and

$$\sum_{j=1}^{4m}\frac{1}{p_j(p_j-\beta_{11})}c_j\mathbf{x}_j=\mathbf{0}, \qquad \sum_{j=1}^{4m}\frac{1}{p_j(p_j-\beta_{21})}c_j\mathbf{x}_j=\mathbf{0}. \tag{15}$$

where the matrices with subscripts in Eqn 14 is associated with  the global stiffness matrix as

$$\mathbf{K}(t)=\mathbf{K_0}+\exp(\beta_{11}t)\mathbf{K_1}+\exp(\beta_{21}t)\mathbf{K_2} \tag{16}$$

Now we can formulate the eigenvalue problem from Eqn 14 by collecting the coefficient matrices of $p_j^{n+2}$, $p_j^{n+1}$, …, $p_j^{0}$ respectively as follows,

$$(p_j\mathbf{A}+\mathbf{B})\mathbf{q}=\mathbf{0} \qquad j=1,\ 2,\ \ldots,\ 4m \tag{17}$$

where **A**, **B** are $4m\times4m$ matrices and **q** is a $4m\times1$ vector defined as in the Ref. 12. From obtained eigenvalues and eigenvectors one can get coefficients $c_j$, in Eqn 13 by solving the $4m$ simultaneous equations consisting of Eqn 15 and zero initial displacement conditions. Then, the time response can be calculated directly from Eqn 13 without numerical time integration because the solution is presented in closed form.

## NUMERICAL RESULTS AND DISCUSSION

In order to show the convergence of the present numerical procedure, numerical results for a simple example are compared to available analytic solutions. Fig. 2 shows the viscoleastic critical loads of a simply supported column under an constant axial force with viscoelastic material property expressed in three parameter solid form, where $P_e$ denotes Euler buckling load with $E_1$ as Young's modulus. One can see that numerical results from the current numerical analysis are in good agreement with the results in the Ref. 4.
The material properties used for sequential numerical simulation are tabulated in Table 1 and

Table 1. *Material properties*

| |
|---|
| $Q_{11}/Q^0_{22}$=29.3, $Q_{11}/Q^0_{12}$=74.6, $Q_{11}/Q^0_{44}$=169.6, $Q_{11}/Q^0_{55}$=130.7, $f_1(\infty)/f_1(0)$=0.3218, $f_2(\infty)/f_2(0)$=0.3090, $k_s$= 5/6 |

following non-dimensionalized parameters are introduced for simplysity,

$$S^* = l/h,\ t_1^* = (\beta_{11} l^2/h)\sqrt{\rho/Q_{11}},\ t_2^* = (\beta_{21} l^2/h)\sqrt{\rho/Q_{11}},$$
$$T^* = (ht/l^2)\sqrt{\rho/Q_{11}},\ \Omega^* = (p_n l^2/h)\sqrt{\rho/Q_{11}},\ Q^* = ql^2/(Q_{11} I_2). \tag{18}$$

In Fig. 3, the eigenvalue curves of some lowest vibration modes are plotted against magnitude of the follower force ($\alpha$=1) for a [0/90/90/0] beam. When one solves Eqn 17, one gets a set of eigenvalues that consists of 2$m$ damped vibration modes and 2$m$ pure real dissipation modes. In this figure, dissipation modes are omitted for they have no affect on the stability The ordinate $\Omega^*_R/\Omega^*_I$, the ratio of the real part to the imaginary part of the complex frequency, denotes the intensity of instability as in the Ref. 13. When the value of the ratio is zero, the system becomes neutrally stable and with the sign of the ratio changing it turns dynamically unstable wherein the amplitude of the vibration is unbounded. As the magnitude of the follower force is increased, instability occurs before the critical load predicted through elastic analysis is reached. While the first vibration mode gets more stable, by the transition of the second mode eigenvalue into the unstable region the system become unstable and it is accompanied by the third and fourth mode in more increased load range. As one can see, the curve indicating second vibration mode approaches the curve of elastic case asymptotically. When the instability considering viscoelastic effect occurs, the intensity of instability is weaker by far than that of the case without considering viscoelasticity and it grows up to the level of elastic instability. So it appears useful to define the level of instability according to the magnitude of $\Omega^*_R/\Omega^*_I$.

For parametric studies, the slenderness ratio and the length of the beam are taken to investigate the effect of geometric conditions in given material properties. First, the effect of the slenderness ratio on the non-dimensionalized critical load for a [0/90/90/0] beam is shown in Fig. 4, where the solid line and the dashed line denote viscoelastic and elastic critical load respectively. In small slenderness ratio region $S$<20 both non-dimensionalized critical loads increase but when $S$>20 viscoelastic critical load decreases while elastic one remains increasing. And in the region between the two critical loads, levels of the instability strength are also divided into two groups, one increasing and the other decreasing. This means that the slenderer the beam is, the larger the range of instability and the stronger the intensity of

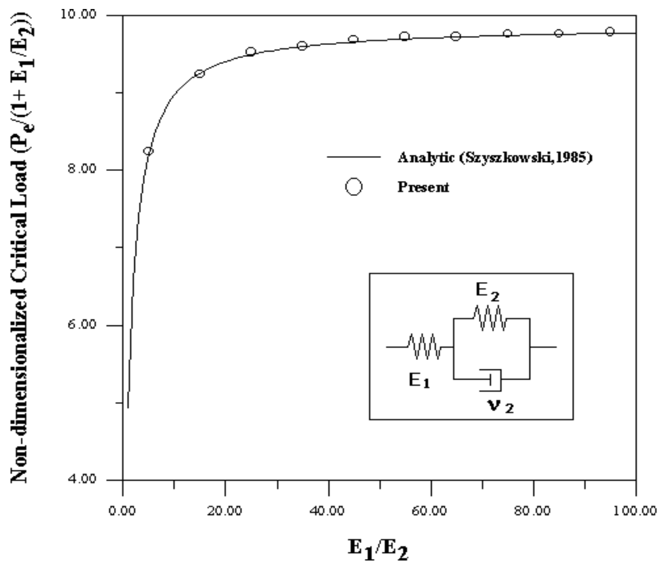

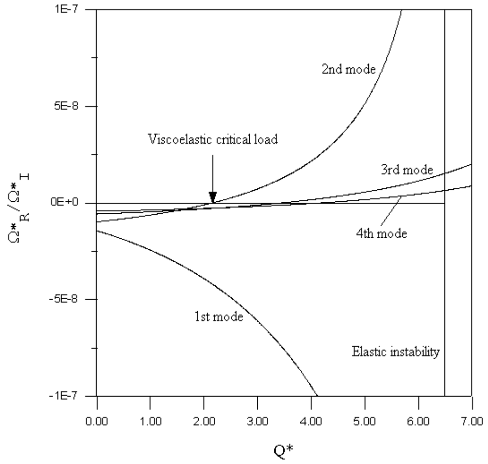


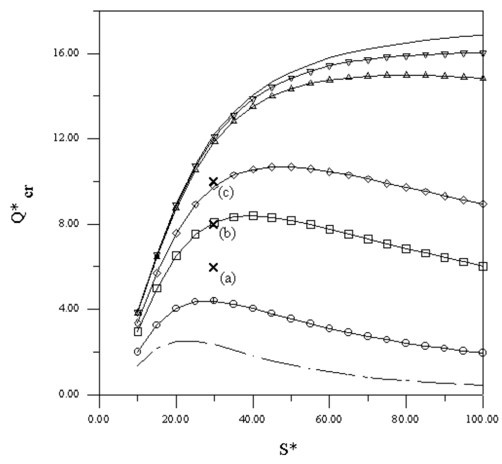


instability becomes.

Fig. 5(a) shows the critical load dependence characteristics with respect to various stacking sequences for elastic case, and Fig. 5(b) for viscoelastic case. In both cases, the [0/90/90/0] and [0/90/0/90] configurations seem to be more dependent on the slenderness ratio than the [0/0/90/90] and [90/0/0/90] configurations.

Secondly, the effect of the length on the non-dimensional critical load of the [0/90/90/0] beam is investigated in Fig. 6. When the elastic stability analysis is performed on this problem, the slenderness ratio is the only geometric parameter that is incorporated in non-dimensionalized governing equations. But, the viscoelastic stability analysis introduces one more geometric parameter in the non-dimensional governing equations, length of the beam, considering that, $t^*_1$, $t^*_2$ in Eqn 19 include the length of the beam as one of the factors. Therefore, one may deal with the effect of the length independently of that of the slenderness ratio by examining the stability characteristics according to the viscoelastic parameters $t^*_1$, $t^*_2$. The critical loads and the intensity of instability dependence on the time constant $t^*_1$ is shown in this figure. Though it seems that $t^*_1$ is taken as a independent variable apart from $t^*_2$, it should be recognized that

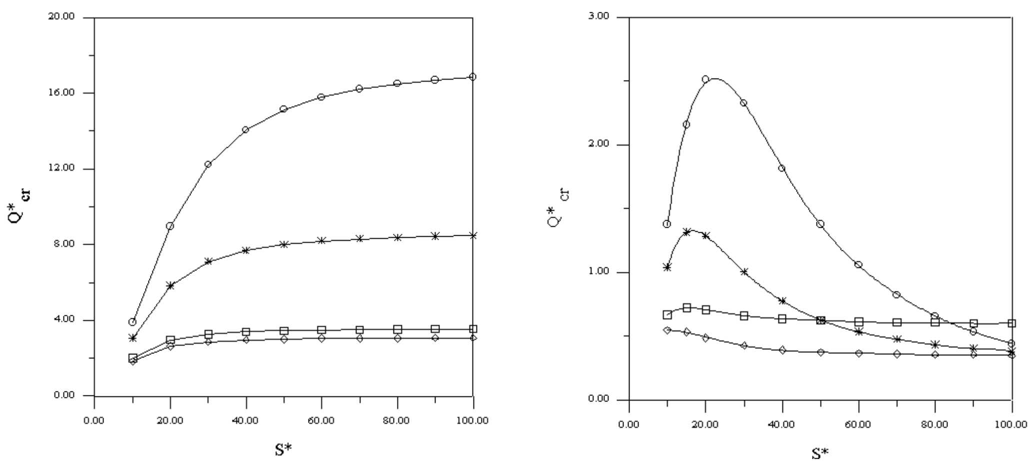

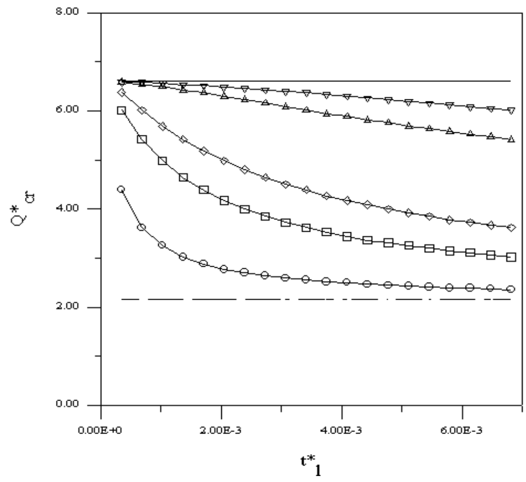


two viscoelastic parameters are in simultaneous consideration. For the length of the beam is the common factor of them as is described. The length does not affect the critical load but increment of the length causes the system to be in more unstable state by extending the stronger instability range.

Finally, strength of the instability is studied through examining the time response of tip deflection under dynamic disturbance for each instability level. Different from the elastic case, even after the occurrence of the instability due to viscoelasticity, the structure can serve without excessive deformation for a certain period safely because compared with the intensity of the elastic instability, that of viscoelastic one is weaker by far. Such a safe service period may be referred to as critical time. One may define this period, as the time required for the response amplitude to become equal to the magnitude of the initial disturbance [4]. Fig. 7 shows the time responses of tip defection during the critical time when the beam is disturbed laterally by velocity field in the shape of the first bending mode at different instability levels (see Fig. 4). From this figure it may be noticed that there exists a period during which the vibration is damped and then the response starts to grow and become unbounded as the non-dimensionalized time $T^*$ tends to infinity. This phenomenon can be explained from Fig. 2 that shows that the instability is caused mostly by the divergence of the second bending mode in

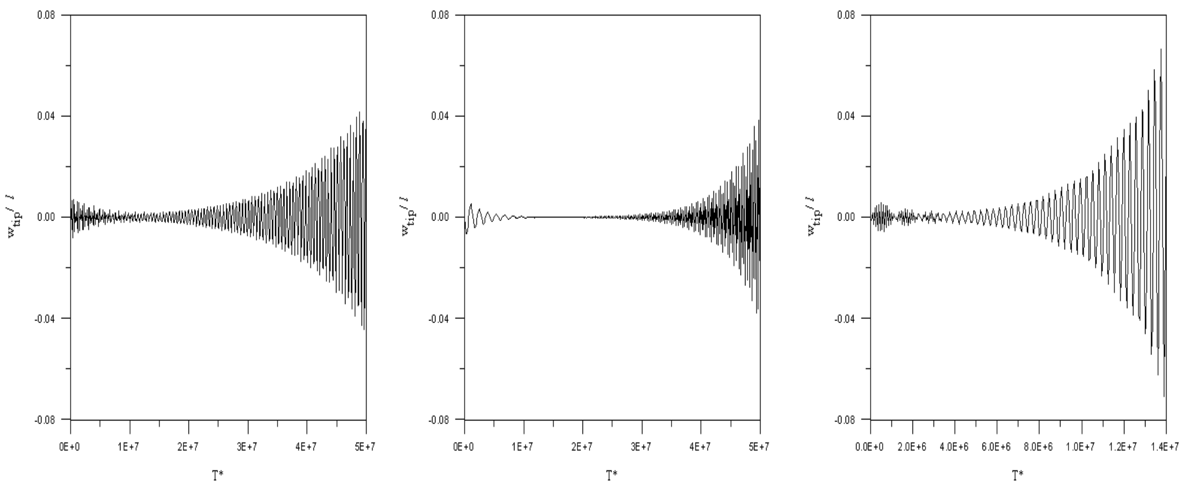

contrast to the stabilization of the first bending mode. Because the first bending mode dominates the vibration of the beam, following enough decrease of first bending mode the unbounded response contributed to by the second bending mode appears. Thus a system that seems to be stable initially can turn unstable after a finite time.

## CONCLUSIONS

In this study, the stability behavior of a laminated cantilever beam subjected to a follower force has been examined numerically considering the viscoelasticity of composite. The following conclusions have been arrived at for the cases considered: (a) The effect of the viscoelasticity reduces the critical load predicted through elastic analysis to viscoelastic critical load lower than the elastic one. (b) As the slenderness ratio of the beam is increased the non-dimensionalized magnitudes of the elastic critical load increases and that of the viscoelastic one decreases. (c) The increment of the viscoelastic parameters or length, when given material properties, leads to growth of the intensity of the instability though they do not affect the critical load. (d) When the instability occurs, there exists a period when the vibration is damped out due to the characteristics of the follower force.

## REFERENCES

1. Shapery, R.A., “Viscoelastic Behavior and Analysis of Composite Materials”, *Composite Materials*, Sendeckyj, G.P, Ed., Academic Press, New York, 1974, pp. 86-167.

2. Stevens, K.K., “On the Parametric Excitation of a Viscoelastic Column”, *American Institute of Aeronautics and Astronautics Journal*, Vol. 4, 1966, pp. 2111-2116.

3. Plaut, R.H., “Instability of a Viscoelastic Cantilever Under a Follower Load”, *Journal of Applied Mechanics*, No. 4, 1971, pp. 1044-1047.

4. Szyszkowski, W. and Glockner, P.G., “The Stability of Viscoelastic Perfect Cloumns: A Dynamic Approach”, *International Journal of Solids and Structures*, Vol. 21, No. 6, 1985, pp. 545-559.

5. Vinogradov, A.M., “Buckling of Viscoelastic Beam Columns”, *American Institute of Aeronautics and Astronautics Journal*, Vol. 25, No. 3, 1987, pp. 479-483.

6. Chandiramani, N.K., Librescu, L. and Aboudi, J., “The Theory of Orthotropic Viscoelastic Shear Deformable Composite Flat Panels and their Dynamic Stability”, *International Journal of Solids and Structures*, Vol. 25, No. 5, 1989, pp. 465-482.

7. Cederbaum, G., Aboudi J. and Elishakoff, I., “Dynamic Instability of Shear-Deformable Viscoelastic Laminated Plates by Lyapunov Exponents”, *International Journal of Solids and Structures*, Vol. 28, No. 3, 1991, pp. 317-327.

8. Yi, S. and Hilton, H.H., “Dynamic Finite Element Analysis of Viscoelastic Composite Plates in the Time Domain”, *International Journal for Numerical Methods in Engineering*, Vol. 37, 1994, pp. 4081-4096.

9. Chandrashekhara, K. and Bangera, K.M., “Free Vibration of Composite Beams Using a Refined Shear Flexible Beam Element”, *Computers and Structures*, Vol. 43, No. 4, 1992, pp. 719-727.

10. Chen, T.M., “The Hybrid Laplace Transform/Finite Element Method Applied to the Quasi-Static and Dynamic Analysis of Viscoelastic Timoshenko Beams”, *International Journal for Numerical Methods in Engineering,* Vol. 38, 1995, pp. 509-522.

11. Yi, S. and Hilton, H.H., “Nonlinear Thermo-Viscoelastic Analysis of Interlaminar Stresses in Laminated Composites”, *Journal of Applied Mechanics,* Vol. 63, 1996, pp. 218-224.

12. Muravyov, A. and Hutton, S.G., “Closed-Form Solutions and the Eigenvalue Problem for Vibration of Viscoelastic Systems”, *Journal of Applied Mechanics,* Vol. 64, 1997, pp. 684-691.

13. Higuchi, K. and Dowell, E.H., “Effect of Structural Damping on Flutter of Plates with a Follower Force”, *American Institute of Aeronautics and Astronautics Journal,*, Vol. 30, No. 3, 1992, pp. 820-825.